nature physics

SUPPLEMENTARY INFORMATION

DOI: 10.1038/NPHYS2380

Decrease of upper critical field with underdoping in cuprate superconductors

SAMPLES

Single crystals of $La_{1.8-x}Eu_{0.2}Sr_xCuO_4$ (Eu-LSCO) were grown by the travelling floating zone method in Tokyo. The hole doping p is taken to be the nominal Sr concentration x. The characteristics of our four samples are listed in Table S1. The superconducting transition temperature T_c was determined as the temperature below which the resistivity $\rho = 0$. For each sample, three pairs of silver epoxy contacts were diffused into the surface. Contacts used to measure the temperature gradient were separated by a distance L and the transverse contacts used to measure the Nernst voltage were separated by a distance w. The ratio L/w was typically in the range 0.5 - 3.

Single crystals of $La_{1.6-x}Nd_{0.4}Sr_xCuO_4$ (Nd-LSCO) used for determining H_{c2} from the resistivity (Fig. S6) were described in ref. 30; the T_c and H_{c2} values are given in Table S1.

	$p = x$	T_c (K)	H_{c2} (T)
Eu-LSCO	0.08	3.6 ± 0.1	9.4 ± 0.9
	0.10	5.0 ± 0.1	7.8 ± 0.7
	0.11	3.86 ± 0.05	6.2 ± 0.5
	0.125	6.5 ± 0.2	12 ± 2
Nd-LSCO	0.12	7.0 ± 0.5	12
	0.20	20.5 ± 0.5	35

TABLE S1 | Sample characteristics.

Strontium concentration x, doping p, superconducting transition temperature T_c (from $\rho = 0$), upper critical field H_{c2}, for the four samples of $La_{1.8-x}Eu_{0.2}Sr_xCuO_4$ (Eu-LSCO) used in this study. The H_{c2} values listed here for Eu-LSCO are simply the values of H_{c2}^*, the parameter in the fit of the peak field H^* vs temperature (Fig. 3): $H^* = H_{c2}^* \ln(T/T_c)$. The error bar on H_{c2}^* corresponds to the upper and lower bounds on the fit above $\varepsilon = 0.5$, given the error bars on H^* (see Fig. 2). We also include the value of H_{c2} measured directly from the resistivity at $T << T_c$ on two samples of Nd-LSCO, a material very similar to Eu-LSCO (see Fig. S6).

NERNST DATA ON Eu-LSCO SAMPLES

In Fig. S1, the Nernst data measured on our four Eu-LSCO samples are displayed both as N vs H (bottom panels) and as ν vs H on a log-log scale (top panels).

NERNST SIGNAL FROM QUASIPARTICLES

Quasiparticles make a sizable contribution to the Nernst signal in underdoped cuprates, which cannot in general be assumed negligible. This has been shown for $Pr_{2-x}Ce_xCuO_{4-d}$ (PCCO) [35] and Eu-LSCO [32], where a positive quasiparticle peak distinct from the superconducting peak is resolved in the Nernst coefficient ν(T), and for YBCO [33, 36], where the quasiparticle contribution is negative, making it immediately distinguishable from the positive superconducting signal.

To obtain the quantity of interest here, N_{sc}, we need to know this quasiparticle contribution N_{qp}, to be subtracted from the measured N (= N_{sc} + N_{qp}). We estimate N_{qp} by applying a magnetic field $H >> H_{c2}$, at which point $N \approx N_{qp}$. In Fig. 2a, we show Nernst data for Eu-LSCO at p = 0.125. At T > 35 K, ν(T) is independent of magnetic field, so that ν ≈ ν_{qp} [32]. Above 35 K, the data for ν / T is perfectly linear up to 70 K: $\nu_{qp} / T = a - bT$. To estimate ν_{qp} for T < 35 K, we applied magnetic fields up to 28 T. We see that ν(28 T) / T is a smooth continuation of the high-temperature behavior. We conclude that the normal-state non-superconducting behavior of the Nernst coefficient is $\nu_{qp} \approx T (a - bT)$ down to the lowest temperatures. This is the curve shown in Fig. 4b, labeled "ν_{qp}". The same fitting procedure is applied to the data at other dopings, giving $\nu_{qp} = T (a - bT)$ in all cases, with slightly different values of a and b.

SIGNAL-TO-BACKGROUND RATIO

Having estimated the quasiparticle component ν_{qp}, we can evaluate the ratio of superconducting signal to non-superconducting background, namely $\nu_{sc} / \nu_{qp} = N_{sc} / N_{qp}$, where $N_{sc} = N - N_{qp}$. For Eu-LSCO at p = 0.11, we find $N_{sc} / N_{qp} \approx 100$ at $T = 1.5\ T_c$ (see Fig. 4b, where $\nu_0 / \nu_{qp} \approx 100$ at ε = 0.5). This "signal-to-background" ratio is 5 orders of magnitude larger than in YBCO at the same doping [33, 36, 37]. In

Table S2, we list the signal-to-background ratio in several previous studies of superconducting fluctuations in cuprates, with various techniques including magnetization and magneto-conductivity, evaluated at the same reduced temperature, namely T / T_c = 1.5. Our Nernst study on Eu-LSCO has a signal-to-background ratio that is at least 100 times larger than all previous studies we are aware of. For other Nernst studies, we could only estimate N_{sc} / N_{qp} reliably for YBCO and PCCO, where N_{qp} is well characterized. However, it is clear that N_{sc} / N_{qp} is also very high in Bi-2201 [20, 38], allowing us to make use of Bi-2201 data in Fig. 7.

If ν_{qp} is unknown, one can get a rough idea of its magnitude (but not its sign) by evaluating $S \tan\theta_H / H$, the product of the Seebeck coefficient, $S = \alpha_{xx} / \sigma_{xx}$, and the tangent of the Hall angle, $\tan\theta_H = \rho_{xy} / \rho$, the ratio of the Hall resistivity ρ_{xy} to longitudinal resistivity ρ [29, 36]. In Table S3, we give the value of $|S \tan\theta_H / H|$ for Eu-LSCO, YBCO and PCCO, evaluated at $T = T_c$. In Eu-LSCO, ν_{sc} is 5 x 10^5 times larger than $|S \tan\theta_H / H|$, while in YBCO it is only ≈ 30 times larger [37].

The very small value of $S \tan\theta_H$ relative to N is what makes it possible to write the Nernst signal as a sum of two separate contributions, $N = N_{sc} + N_{qp}$, because the 2nd term in the defining expression for the Nernst effect, $N = \alpha_{xy} \rho_{xx} - \alpha_{xx} \rho_{xy}$ [29], can be neglected, so that $N_{sc} \approx \alpha_{xy}^{sc} \rho_{xx}$ and $N_{qp} \approx \alpha_{xy}^{qp} \rho_{xx}$. This remains true even in the range 10 K < T < 30 K, where N_{sc} and N_{qp} have comparable magnitude (see Fig. 2). At T = 20 K, for example, even though N is 50 times smaller than at T_c, S has grown by at most a factor 10 (from $S \sim T$) and $\tan\theta_H$ has remained roughly constant, so that $|N / S \tan\theta_H| \approx 1000$.

Nernst effect	Material	Doping	T_c (K)	N_{sc}/N_{qp}	Ref.
	Eu-LSCO	**0.11**	**3.86**	**100**	**This work**
	YBCO	0.12	66	< 0.01	(37)
	YBCO	0.10	57	< 0.01	(36)
	PCCO	-0.13	12	< 0.1	(35)
Diamagnetism				$-M_d/M_p$	
	LSCO	0.09	24	< 1	(20)
	Bi2201	UD	12	< 1	(20)
	Bi2212	UD	50	< 1	(21)
	YBCO	~ 0.16	92	0.1	(20)
Magneto-conductivity				$\Delta\sigma_{sc}/\sigma$	
	$La_{2-x}Sr_xCuO_4$	0.12-0.13	$\sim$30	$< 1^*$	(49)
	YBCO	0.07-0.18	35-90	$< 0.01^*$	(7)
	YBCO	0.10	57	$< 0.05^*$	(39)
Paraconductivity				σ_{sc}/σ_{qp}	
	LSCO	0.10-0.12	25-30	< 1	(43)
	B2201	0.11-0.18	20-30	< 1	(43)
	$Bi_2Sr_2CaCu_3O_8$	-	85	< 0.1	(44)
	$Bi_2Sr_2CaCu_3O_{10}$	0.16	105	0.1	(44)
	YBCO	0.12	60	< 1	(43)
	YBCO	-	90	0.1	(44)
Microwave absorption				$\Delta R_s/R_s$	
	YBCO	0.10	57	< 0.01	(41)
	Hg1201	0.16	94	< 0.01	(42)
THz Spectroscopy				σ_{sc}/σ_{bck}	
	LSCO	0.12	35	< 0.01	(45)
	LSCO	0.16	40	< 0.01	(45)
Specific heat				γ_{sc}/γ_{bck}	
	Bi2201	$\sim 0.12 - 0.20$	10-30	< 1	(46)
	Y124	~ 0.14	$\sim$80	< 0.01	(47)
Thermal expansion				$\alpha_{elec.}/\alpha_{bck}$	
	YBCO	$\sim 0.13 - 0.18$	80-93	< 0.1	(48)

* This value was obtained by evaluating data taken at a field of 10 T.

TABLE S2 | Signal-to-background ratio.

Ratio of superconducting contribution to non-superconducting background in various properties (left column) on a variety of cuprate materials (labelled in second column). The ratio is evaluated at the same temperature relative to T_c, namely T = 1.5 T_c (penultimate column). The relevant data can be found in the cited reference (last column). The doping and T_c values are listed; in some cases, the doping of underdoped (UD) samples was not given. (LSCO = $La_{2-x}Sr_xCuO_4$; Bi-2223 = $Bi_2Sr_2Ca_2Cu_3O_{10}$; Y-124 = $YBa_2Cu_4O_8$; Hg-1201 = $HgBa_2CuO_{4+\delta}$.)

Compound	x	T_c	ν_{sc}	$\frac{\lvert S\rvert \tan\theta}{H}$	$\frac{\nu_{sc}H}{\lvert S\rvert \tan\theta}$	Ref.
		(K)	(μV/K T)	(μV/K T)		
Eu-LSCO	0.11	3.86	2	4×10^{-6}	5×10^{5}	This work
YBCO	0.12	66	0.3	0.01	30	(37)
PCCO	0.13	11.8	2.4	0.007	340	(35)
$Nb_{0.15}Si_{0.85}$	-	0.38	3	0.5×10^{-6}	6×10^{6}	(11)

Table S3 | Estimate of quasiparticle contribution to the Nernst effect.

Comparison of the measured Nernst coefficient ν, at $H \rightarrow 0$, with the quantity $S \tan\theta_H / H$, a common estimate of ν_{qp}, the quasiparticle contribution to ν (see text). Both values are given for different superconductors, evaluated at $T = T_c$, with doping and T_c values as indicated. Their ratio, $|N / S \tan\theta_H|$, is given in the penultimate column.

ADVANTAGES OF STUDYING Eu-LSCO

A powerful study of superconducting fluctuations requires that the fluctuations be tracked to temperatures well above T_c and magnetic fields well above H_{c2}. Given the limits on static fields accessible in the laboratory (typically 15 T, perhaps 30 T, at most 45 T), it is an advantage to work with a material that has a low H_{c2}. This is the case of PCCO, where $H_{c2} < 10$ T [35], but also of Eu-LSCO, where $H_{c2} \approx 6 - 12$ T (Table S1). By contrast, YBCO has $H_{c2} > 25$ T for all $p > 0.07$ (Fig. 5b).

For high resolution, it is an advantage to work with the largest possible signal. Since $N_{sc}\ \sigma \sim \xi_0^2 / T \ln(T/T_c)$ (see theory section below), the absolute magnitude of the superconducting Nernst signal N_{sc} at a given value of T / T_c is proportional to $\rho / (H_{c2} T_c)$. So here again Eu-LSCO is ideal: not only does it have a low H_{c2} and a low T_c, but it has a high resistivity ρ. In comparison to YBCO at $p = 0.11$ (whose resistivity is 10 times lower), the three factors combine to produce a signal that is 1000 times larger in Eu-LSCO.

But the principal difficulty with studies of superconducting fluctuations, whose amplitude decreases with increasing T / T_c, is the quasiparticle background, which increases with T. The third and main advantage of Eu-LSCO is its exceptionally large signal-to-background ratio, at least 100 times larger than all previous studies we are aware of (see Table S2). The Nernst signal from quasiparticles, N_{qp}, grows roughly as the product of mobility and temperature [29], *i.e.* as (ρ_{xy} / ρ) T, so that for a given value of T / T_c, N_{qp} is proportional to T_c / ρ. This gives a ratio N_{sc} / N_{qp} which goes roughly as ρ^2 / (H_{c2} T_c^2). Compared to YBCO, this gives Eu-LSCO an extra factor of 100 to the previous 1000, for a combined advantage of 10^5.

All this is only useful if Eu-LSCO is representative of hole-doped cuprates. This is indeed the case. Our Nernst measurements of the superconducting fluctuations, previous Seebeck measurements of the normal state [24, 37] and recent characterizations of the stripe order [26, 27] all reveal a fundamental similarity between Eu-LSCO and YBCO.

PEAK FIELD (or "ghost critical field")

Effect of quasiparticle contribution

The Nernst signal from superconducting fluctuations N_{sc} decreases as the temperature is raised away from T_c. At the same time, the quasiparticle contribution N_{qp} increases. To extract the "ghost critical field" H^* (the peak in N_{sc} vs H) far away from T_c, it is therefore necessary to subtract N_{qp} from the measured Nernst coefficient N. The effect of this subtraction is illustrated in Fig. 2b. For $\varepsilon < 1$, the determination of H^* is essentially unaffected by the subtraction of N_{qp}. By contrast, for $\varepsilon > 1$, an accurate value of H^* can only be obtained once $N_{qp} = \nu_{qp}(T)\ H$ has been subtracted. The uncertainty in $\nu_{qp}(T)$, illustrated as upper and lower bounds in Fig. 2a, yields an error bar on H^*, plotted on the data of Figs. 3b and 3c.

Effect of paraconductivity

While having a good estimate of N_{qp} may be less of an issue in the regime $\varepsilon < 1$, there is another complication in that regime, close to T_c: paraconductivity – the contribution of superconducting fluctuations to σ. This is because the experimentally measured quantity, the Nernst signal N, is the ratio of two fundamental quantities, namely the Peltier coefficient α_{xy} and the electrical conductivity σ: $N = \alpha_{xy} / \sigma$. These two quantities both diverge as $T \rightarrow T_c$ ($\alpha_{xy} \sim \varepsilon^{-1}$ and $\sigma \sim \varepsilon^{-1}$ [13]), but their ratio remains relatively constant (see Fig. 4). Now it is α_{xy}, and not N, which is directly related to ξ_0^2 [13, 14, 15], and hence to H_{c2}, the quantity of interest. Near T_c, both α_{xy} and σ have strong field dependence, and so the field dependence of α_{xy} is significantly different from that of N. In particular, the peak field H^*_α in α_{xy} is lower than the peak field H^* in N. At temperatures away from T_c, when paraconductivity becomes negligible compared to the normal-state background, then the H dependence of α_{xy} and N_{sc} become the same, and the physically meaningful peak field H^*_α can be reliably extracted from the measured N_{sc}.

In Fig. 3b, we see that H^* obtained from N_{sc} vs H deviates from $\ln(T / T_c)$ below $\varepsilon \approx 0.5$. In Fig. S4, we show how taking into account the field-dependent σ corrects for that deviation. It leads to a lowering of H^* close to T_c, in a way that makes H^* converge to the relation

$$H^* \sim \ln(T / T_c)$$

at low values of ε.

As a result of this effect, using Nernst isotherms (N_{sc} vs H) close to T_c, or at T_c , as done in ref. 8, to extract a field scale characteristic of superconductivity will lead to spurious results. In Figs. 1b and 7, we show how the same Nernst data on Bi-2201 (from ref. 10) yield a field scale that *rises* with underdoping when data at T_c are used, but a field scale that *drops* with underdoping when data at $T/T_c > 1.5$ are used. Magnetization data on the same material (from ref. 20) confirm that the latter approach gives the correct values and doping dependence of H^* (see next section).

PRIOR STUDIES OF SUPERCONDUCTING FLUCTUATIONS IN CUPRATES

Diamagnetism

Superconductivity causes a strong diamagnetic response. Above T_c, superconducting fluctuations contribute a (negative) diamagnetic component, M_d, to the measured magnetization M, which reduces M from its paramagnetic (positive) background, M_p: $M_d = M - M_p$. Torque measurements have been used to study superconducting fluctuations in the magnetization of cuprates [20, 21]. Note that away from T_c, the signal-to-background ratio tends to be relatively small, namely $-M_d / M_p < 1$ at $T/T_c = 1.5$, compared to $N_{sc} / N_{qp} = 100$ in Eu-LSCO (Table S2). On the other hand, M_d is not contaminated by paraconductivity and can thus be used directly close to T_c.

Isotherms of $-M_d$ vs H are very similar to isotherms of N_{sc} vs H [21], as also found in several theories where $N_{sc}\,\sigma \sim -M_d$ [16, 22]. One can therefore define a peak field, H_d^*, in the diamagnetic signal. In Fig. 7, we plot H_d^* vs ε obtained from published magnetization data on Bi-2201 [20]. It is seen to obey the relation

$$H_d^* = H_{c2}^* \ln(T / T_c) \quad ,$$

over the entire temperature interval available, e.g. from $T \approx T_c$ to $T \approx 4\ T_c$ in the underdoped sample. Above $\varepsilon \approx 0.5$, $H_d^* \approx H^*$, so that both M_d and N_{sc} directly yield the same field scale H_{c2}^*. Note that this field scale, *i.e.* H_{c2}^* from M_d, *rises* with increased doping (Fig. 1b).

In summary, both diamagnetic and Nernst signals in the cuprate Bi-2201 obey the relation $H^* = H_{c2}^* \ln(T / T_c)$, from which the same field scale can be reliably extracted, and this field scale (proportional to H_{c2}) decreases with underdoping (Fig. 1b). This resolves the apparent contradiction highlighted in Fig. 1a.

Note that in prior work, H_{c2} was defined as the field where M_d vs H goes to zero [20]. There is no theoretical justification for such a definition, based on the notion that as long as there are detectable fluctuations then $H < H_{c2}(T)$ – suggesting that H_{c2} is very high in underdoped cuprates. Fluctuations never actually go to zero, and in practice this H_{c2} turns out to be the field where the diamagnetic signal becomes too small to be

resolved from the background. In underdoped Bi-2201 with T_c = 12 K, this turns out to be ≈ 45 T. Roughly the same field would be obtained at optimal doping (see ref. 20).

Nernst effect

In ref. 8, isotherms of N vs H at $T = T_c$ in two cuprates (Bi-2201 and Bi-2212) were shown to collapse onto a single curve when plotted as N vs H/H_0, where H_0 is some field scale. That field scale H_0 was found to rise when the doping is reduced from overdoped to underdoped, for both materials. This seemed to be a compelling argument that the pairing strength, proportional to that field scale H_0, must increase as the cuprates become underdoped. However, if the same analysis is carried out at some other temperature, say T = 1.5 T_c, the opposite conclusion is reached: the characteristic field scale for superconductivity *decreases* as cuprates become underdoped (see Figs. 7 and 1b). The reason for the discrepancy lies in the fact that N is the ratio of two quantities, α_{xy} and σ, which both diverge as $T \rightarrow T_c$. The Nernst data at T_c is thus a combination of two rapidly changing functions of H, so that the field scale characteristic of α_{xy} vs H is convoluted with the field-dependent paraconductivity. At higher T, when σ becomes essentially independent of H, N_{sc} vs H has the same field profile, and hence the same characteristic field scale, as α_{xy} vs H. The same field scale is obtained from diamagnetism data (see previous section and Fig. 1b). And that field scale *decreases* with underdoping.

As done with magnetization data (see previous section), H_{c2} has also been defined as the field where N vs H goes to zero [8]. This is again based on the notion that as long as there are detectable fluctuations, then $H < H_{c2}(T)$. In underdoped Bi-2201 with T_c = 12 K, this definition yields "H_{c2}" ≈ 65 T [8]. This is larger than the value of ≈ 45 T determined in the same way from M_d vs H (previous section), probably because the signal-to-background ratio is larger in the Nernst data, enabling fluctuations to be tracked further in field. By comparison, the well-defined value of H_{c2}* obtained by fitting the peak field H* vs T/T_c, whether from N_{sc} or from M_d, is H_{c2}* ≈ 19 T (for Bi-2201 with T_c = 12 K).

Magneto-conductivity

Upon approaching T_c from above, the zero-field resistivity drops increasingly below its normal-state value due to superconducting fluctuations, a phenomenon called paraconductivity. This drop is attenuated by application of a magnetic field to suppress the fluctuations, which leads to a positive magneto-resistance (MR) that adds to the normal-state transport. Ando and Segawa carried out a detailed analysis of the MR in YBCO as a function of temperature for a wide range of doping [7]. They assume that the normal-state MR observed at high temperature would extend down to $T = T_c$ in the absence of fluctuations, and assign the remaining MR to superconducting fluctuations. They fit the resulting fluctuation magneto-conductivity $\Delta\sigma / \sigma$ to Gaussian (Aslamazov-Larkin) theory and extract a coherence length ξ_0 vs p, and then plot the doping dependence of $H_{c2} = \Phi_0/2\pi\xi_0^2$, as reproduced in Fig. 1a (and Fig. 5).

There are two key findings: 1) H_{c2} decreases dramatically in going from optimal doping to underdoped, namely from $H_{c2} \approx 300$ T at $p = 0.16$ ($T_c = 93$ K) to $H_{c2} \approx 25$ T at $p = 0.06$ ($T_c = 25$ K); 2) this decrease is not monotonic – it shows a minimum at $p = 0.11$ ($T_c = 60$ K), where $H_{c2} \approx 35$ T.

Note that the signal-to-background ratio is very small: at $T / T_c = 1.5$ (in $H = 10$ T), $\Delta\sigma / \sigma < 0.01$ at $p = 0.11$ and $\Delta\sigma / \sigma < 0.0001$ at $p = 0.16$ [7]. The analysis therefore depends critically on the precise form of the magneto-conductivity assumed for the normal-state background. A second study of fluctuation magneto-conductivity in YBCO reported recently [39] arrives at the same qualitative result that H_{c2} decreases with underdoping, although the actual values of H_{c2} can differ by a factor 2 or so. Transport measurements of the magnetic field needed to suppress superconductivity in YBCO at $T < 10$ K [23, 24] yield values of H_{c2} that are in remarkably good agreement with those extracted by Ando and Segawa from the fluctuations above T_c, at least in the range $0.08 < p < 0.13$ (Fig. 5b) where their signal ($\Delta\sigma / \sigma$) is largest. The fact that this transport H_{c2} also has a minimum at $p = 0.11$ confirms that the coherence length does indeed have a local maximum there, as found here in Eu-LSCO (Fig. 5a).

NERNST EFFECT IN THE CONVENTIONAL SUPERCONDUCTOR $Nb_{0.15}Si_{0.85}$

In the $Nb_{0.15}Si_{0.85}$ films of ref. 11, v_{sc} was 10^6 times larger than $S \tan\theta_H / H$ (Table S3) and superconducting fluctuations were detected by Nernst measurements up to $T = 30\ T_c$ and $H = 5\ H_{c2}$ [11, 12, 17]. These Nernst experiments on $Nb_{0.15}Si_{0.85}$ allowed the extraction of the ghost critical field H^*, defined as the field where N vs H has its maximum. It was found to obey $H^* = H_{c2}^* \ln(T / T_c)$ [12, 17]. The authors explained the ghost critical field as a crossover from a low-field regime where the spatial extent of the superconducting fluctuations is controlled by the coherence length $\xi(T) = \xi_0 / (\ln(T/T_c))^{1/2}$ to a high-field regime where their extent is controlled by the magnetic length $l_B = (\hbar / 2\ e\ H)^{1/2}$ [17]. They then made the ansatz that H^* is given by the condition that $\xi(T) = l_B(H^*)$. This yields $H_{c2}^* = \Phi_0 / 2\pi\xi_0^2 = H_{c2}$, the T=0 upper critical field.

THEORY OF SUPERCONDUCTING FLUCTUATIONS

In 2009, a complete microscopic theory of the Nernst effect due to fluctuations in the superconducting order parameter was developed independently by two groups using different methods [14, 15], for a 2D dirty *s*-wave superconductor. These calculations agree with and extend the previous theory [13] to arbitrary temperatures and magnetic fields, above the $H_{c2}(T)$ line. Here we highlight a few important findings. The first finding is for the temperature dependence of the superconducting Nernst signal in the low field limit ($H \rightarrow 0$), namely [14, 15]:

$$N_{sc}\,\sigma \ \sim\ \xi_0^2 / T \ln(T/T_c)\ .$$

For T/T_c close to 1.0, this reduces to the earlier result [13]: $N_{sc}\ \sigma \sim \xi_0^2 / \varepsilon$, where $\varepsilon = (T-T_c)/T_c$. This predicted temperature dependence agrees very well with Nernst data taken on thin films of the dirty *s*-wave superconductor $Nb_{0.15}Si_{0.85}$, up to $T/T_c \approx 30$ [11, 12, 17]. As shown in Fig. 4d, excellent agreement is also found in Eu-LSCO, a 2D *d*-wave superconductor in the dirty limit. This suggests that although the prefactor may be different, the temperature dependence is the same for *d*-wave and *s*-wave.

It is worth emphasizing that N_{sc} never really goes to zero: fluctuations extend up to

arbitrary temperature. Consequently, it is meaningless to define, as is sometimes done, an "onset temperature" below which fluctuations "start". How high in temperature above T_c fluctuations can be detected by a particular technique is a question of sensitivity and signal-to-background ratio. In $Nb_{0.15}Si_{0.85}$, fluctuations have been tracked in the Nernst signal up to 30 T_c because the signal-to-background ratio is enormous; in Eu-LSCO, we have tracked them up to 6 T_c. In most studies of cuprates, superconducting fluctuations have not been tracked beyond 1.5 T_c.

The implication of this simple theoretical relation for our purpose is that measurements of N_{sc} and σ on one material at different dopings will directly yield the doping dependence of ξ_0^2 (modulo some constant multiplicative factor), *i.e*. the doping dependence of H_{c2}.

A second finding provides an even more direct measure of H_{c2}. The calculated field dependence of N_{sc} σ (= α_{xy}^{sc}) at fixed temperature shows a characteristic peak profile [14, 15, 40] in excellent agreement with experiment on $Nb_{0.15}Si_{0.85}$ [11, 12, 17] and on Eu-LSCO (Fig. 6a). Unpublished calculations [K. Michaeli, private communication] show that not only is the initial slope controlled by ξ_0, but so is the entire curve. In other words, theoretical isotherms at a given T/T_c for different ξ_0 values collapse onto a single curve when plotted vs $H\ D$ (see Fig. S7), where the diffusion constant $D \sim \xi_0^2$ [11]. This collapse is indeed observed in our experimental data on Eu-LSCO (Fig. S8).

It is worth stressing again that N_{sc} never really goes to zero: fluctuations extend up to arbitrary field. Consequently, it is meaningless to define an "onset field" below which fluctuations "start", and there is no justification for identifying such an "onset field" with H_{c2}, as is sometimes done. In $Nb_{0.15}Si_{0.85}$, fluctuations have been tracked in the Nernst signal up to 5 H_{c2} [12, 17]; in Eu-LSCO, we have also tracked them up to 5 H_{c2} (inset of Fig. 6b).

The position of the peak in N_{sc} σ vs H, at H^*_α, is a direct measure of H_{c2}. At temperatures away from T_c, where paraconductivity is negligible and σ is independent of field (see section below on "Peak field – Effect of paraconductivity"), it is sufficient to plot N_{sc} vs H to obtain H^*. In that regime, theory yields a beautifully simple relation:

$$H^*_\alpha = H_{c2}\, f(T/T_c) \ .$$

So by measuring N_{sc} vs H at say T/T_c = 1.5 on Eu-LSCO samples with different dopings, the observed peak field H^* is a direct measure of H_{c2} at each doping, within a constant multiplicative factor. This has the major advantage of relating H_{c2}, the quantity of interest, to a field scale that can be immediately read off the Nernst data, as in Fig. 3a, independent of the absolute magnitude of N_{sc} and independent of the conductivity σ.

Data both on $Nb_{0.15}Si_{0.85}$ [11, 12, 17] and on Eu-LSCO (Fig. 3) show experimentally that

$$f(T/T_c) = A \ln(T/T_c) \ ,$$

where A is a constant. This dependence agrees with theoretical calculations (Fig. S7). As mentioned above, assuming that H^*_α is the field where the magnetic length becomes equal to the coherence length yields $f(T/T_c) = A \ln(T/T_c)$, with A = 1.0 [17]. Then we have:

$$H^*_\alpha = H_{c2} \ln(T/T_c) \ .$$

In this article, we have assumed A = 1.0, so that $H_{c2}^* = H_{c2}$ in Fig. 3, but our conclusions on the doping dependence of H_{c2} are independent of the particular value of A (and indeed of the specific form of $f(T/T_c)$). Note that transport measurements of H_{c2} at $T << T_c$ (Fig. S6) do confirm that the choice of A = 1.0 is justified.

Our Eu-LSCO data are in excellent agreement with three non-trivial signatures of Gaussian fluctuations. The first two are $N_{sc}\, \sigma \sim 1 / T \ln(T/T_c)$ and $H^* \sim \ln(T/T_c)$. The third applies to the low-T high-H region, where theory predicts [14, 15]:

$$N_{sc}\, \sigma \ \sim \ \alpha_{xy}^{sc} \ \sim \ 1 / H \ln(H / H_{c2}) \quad ,$$

for $T \rightarrow 0$ and $H >> H_{c2}(0) \equiv H_{c2}$. In the inset of Fig. 6b, we plot N_{sc} vs H in Eu-LSCO at $T < T_c$ up to H = 34 T. At $H > 1.5\, H_{c2}$, N_{sc} agrees with the theoretical dependence of the theory.

In Figs. S8 and 6b, we see that Nernst isotherms at different dopings collapse onto a single curve when H is normalized by $H_{c2} \equiv \Phi_0 / 2\pi\xi_0^2$ for both $T > T_c$ (Fig. S8) and $T < T_c$ (Fig. 6b). This shows that the H dependence of the fluctuations is controlled by H_{c2}

throughout the phase diagram, just as the T dependence is controlled by the transition temperature T_c. In Fig. S9, we show that not only does $\nu_0 \sigma$ in Eu-LSCO exhibit precisely the temperature dependence expected of Gaussian theory at all dopings, namely $\nu_0 \sigma \sim \xi_0^2 / [(T/T_c) \ln(T/T_c)]$, but the magnitude of $\nu_0 \sigma$ is indeed proportional to ξ_0^2. These are the signatures of Gaussian fluctuations.

REFERENCES

[35] Li, P. & Greene, R. L. Normal-state Nernst effect in the electron-doped $Pr_{2-x}Ce_xCuO_{4-d}$: Superconducting fluctuations and two-band transport. *Phys. Rev. B* **76**, 174512 (2007).

[36] Rullier-Albenque, F. *et al.* Nernst effect and disorder in the normal state of high-T_c cuprates. *Phys. Rev. Lett.* **96**, 067002 (2006).

[37] Chang, J. *et al*. Nernst and Seebeck coefficients of the cuprate superconductor $YBa_2Cu_3O_{6.67}$: A study of Fermi surface reconstruction. *Phys. Rev. Lett.* **104**, 057005 (2010).

[38] Okada, Y. *et al.* Enhancement of superconducting fluctuation under the coexistence of a competing pseudogap state in $Bi_2Sr_{2-x}R_xCuO_y$. *Phys. Rev. B* **81**, 214520 (2010).

[39] Rullier-Albenque, F. *et al.* High-field studies of superconducting fluctuations in high-T_c cuprates: Evidence for a small gap distinct from the large pseudogap. *Phys. Rev. B* **84**, 014522 (2011).

[40] Michaeli, K. & Finkel'stein, A. M. Quantum kinetic approach to the calculation of the Nernst effect. *Phys. Rev. B* **80**, 214516 (2009).

[41] Grbic, M.S. *et al.* Temperature range of superconducting fluctuations above T_c in $YBa_2Cu_3O_{7-\delta}$ single crystals. *Phys. Rev. B* **83**, 144508 (2011).

[42] Grbic, M.S. *et al.* Microwave measurements of the in-plane and c-axis conductivity in $HgBa_2CuO_{4+\delta}$: Discriminating between superconducting fluctuations and pseudogap effects. *Phys. Rev. B* **80**, 094511 (2009).

[43] Ando, Y. *et al*. Electronic phase diagram of high-*Tc* cuprate cuperconductors from a mapping of the in-plane resistivity curvature. *Phys. Rev. Lett*. **93**, 267001 (2004).

[44] Cimberle, M.R. *et al*. Crossover between Aslamazov-Larkin and short-wavelength fluctuation regimes in high-temperature-superconductor conductivity experiments. *Phys. Rev. B* **55**, R14745 (1997).

[45] Bilbro, L. S. *et al*. Temporal correlations of superconductivity above the transition temperature in $La_{2-x}Sr_xCuO_4$ probed by terahertz spectroscopy. *Nat. Phys.* **7**, 298–302 (2011).

[46] Wen, H. H. *et al*. Specific-heat measurement of a residual superconducting state in the normal state of underdoped $Bi_2Sr_{2-x}La_xCuO_{6+\delta}$ cuprate superconductors. *Phys. Rev. Lett.* **103**, 067002 (2009).

[47] Tallon, J. L. Fluctuations and critical temperature reduction in cuprate superconductors. *Phys. Rev. B* **83**, 092502 (2011).

[48] Meingast, C. *et al*. Phase fluctuations and the pseudogap in $YBa_2Cu_2O_y$. *Phys. Rev. Lett.* **86**, 1606 (2001).

[49] Kimura, T. *et al*. In-plane and out-of-plane magnetoresistance in $La_{2-x}Sr_xCuO_4$ single crystals. *Phys. Rev. B* **53**, 8733 (1996).

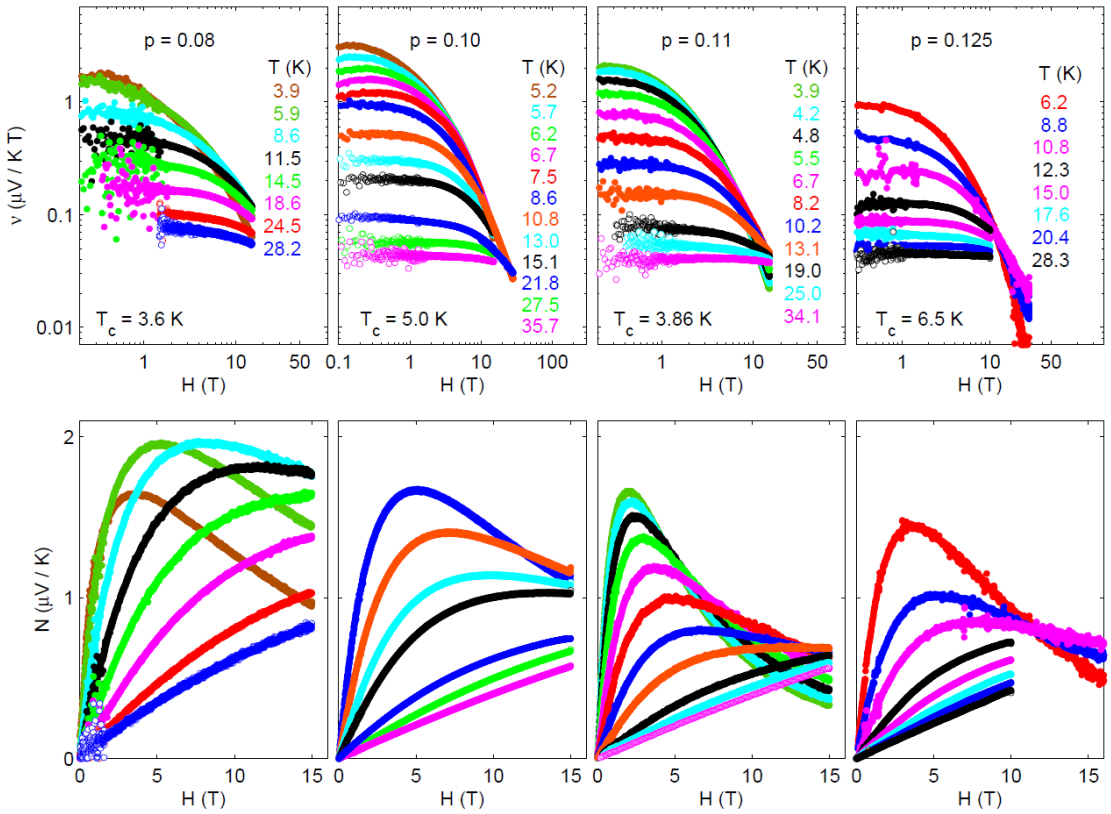

Figure S1 | Nernst data of Eu-LSCO crystals.

Isotherms of ν (top panels) and N (bottom panels) vs magnetic field H for $T > T_c$, in Eu-LSCO with p = 0.08, 0.10, 0.11, and 0.125. The low-field limit of ν in the top panels is plotted vs reduced temperature ε in Figs. 4 and S9. The peak field H^* at which N_{sc} vs H peaks is plotted as a function of ε in Fig. 3c.

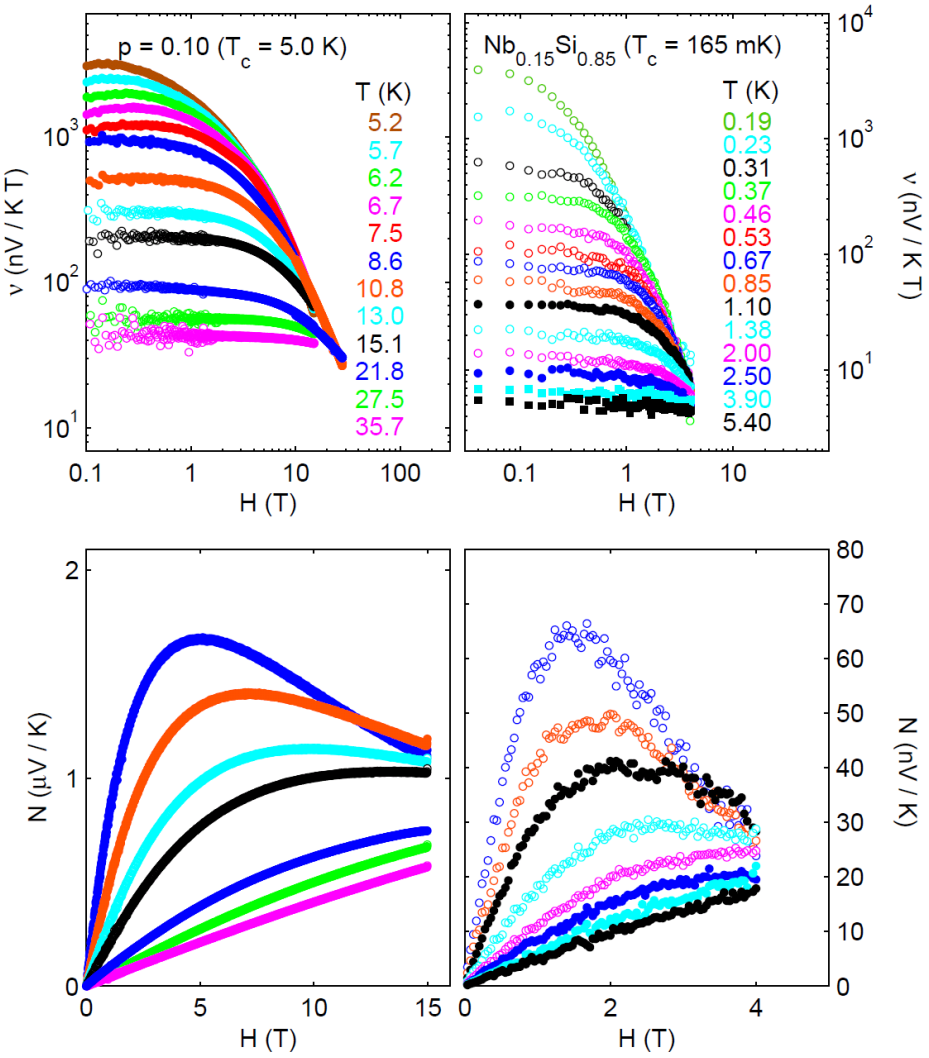

Figure S2 | Comparison of Nernst data in Eu-LSCO and NbSi.

Isotherms of ν (top panels) and N (bottom panels) vs magnetic field H for $T > T_c$, in Eu-LSCO with $p = 0.10$ (this work) and in $Nb_{0.15}Si_{0.85}$ (from refs. 11, 12, 17). In both materials, the low-field limit of ν in the top panels obeys the temperature dependence of Gaussian theory (see Fig. 4d, Fig. S9 and ref. 12) and the peak field H^* at which N_{sc} (= $N - N_{qp}$) vs H peaks obeys the same temperature dependence (see Fig. 3c).

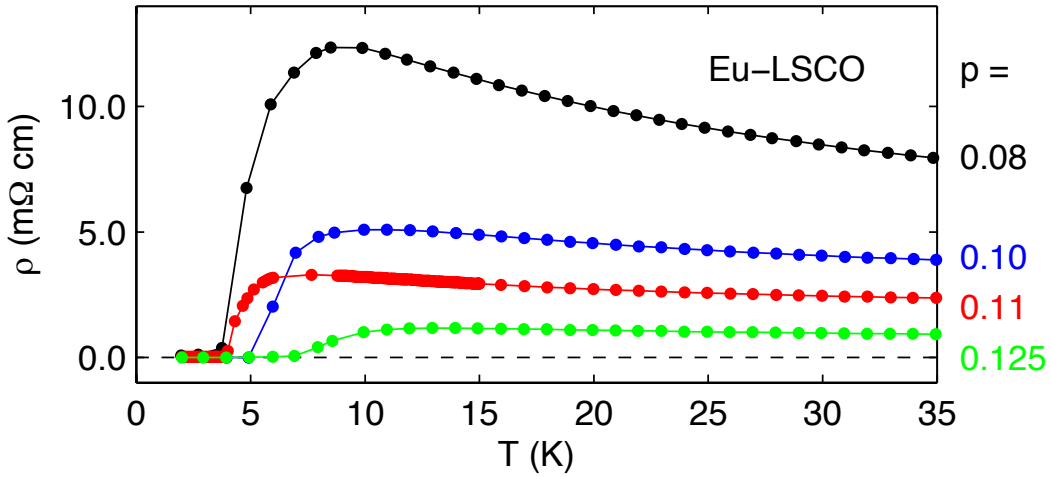

Figure S3 | Electrical resistivity of Eu-LSCO.

In-plane electrical resistivity of our four Eu-LSCO samples in zero magnetic field, for dopings *p* as indicated. The zero-field conductivity σ shown in Fig. 4c is the inverse of this data: σ = 1/ρ.

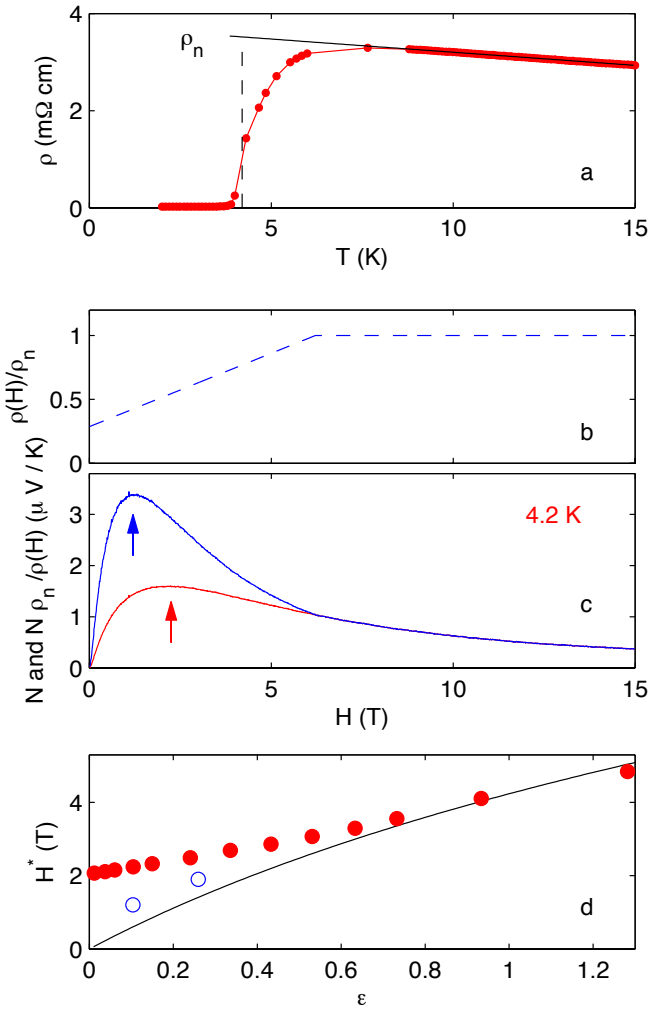

Figure S4 | Impact of *H*-dependent paraconductivity on *H near T_c.**

a) Zero-field resistivity of Eu-LSCO at p = 0.11 (Fig. S3). The normal-state resistivity ρ_n (known to be independent of H) is modeled by assuming that the linear T dependence of $\rho(T)$ above 8 K persists down to 3 K (solid black line). **b)** Idealized field-dependent resistivity ρ(H), assumed to become constant above H_{c2} = 6.2 T, divided by ρ_n, at T = 4.2 K. **c)** Nernst isotherm at T = 4.2 K, plotted as N vs H (blue curve) and as $N\,\rho_n / \rho(H)$ vs H (red curve). Given that $\alpha_{xy} \propto N\,\rho_n / \rho(H)$, the H dependence of ρ makes the ghost critical field H^* extracted from α_{xy} vs H (blue arrow) lower than that extracted from N vs H (red arrow). This effect becomes negligible for $T > 1.5\ T_c$ or so ($\varepsilon > 0.5$), when the resistivity becomes essentially field independent ($\rho \approx \rho_n$). **d)** H^* extracted from N vs H (red circles; Fig. 3b) and from $N\,\rho_n / \rho(H)$ vs H (open blue circles).

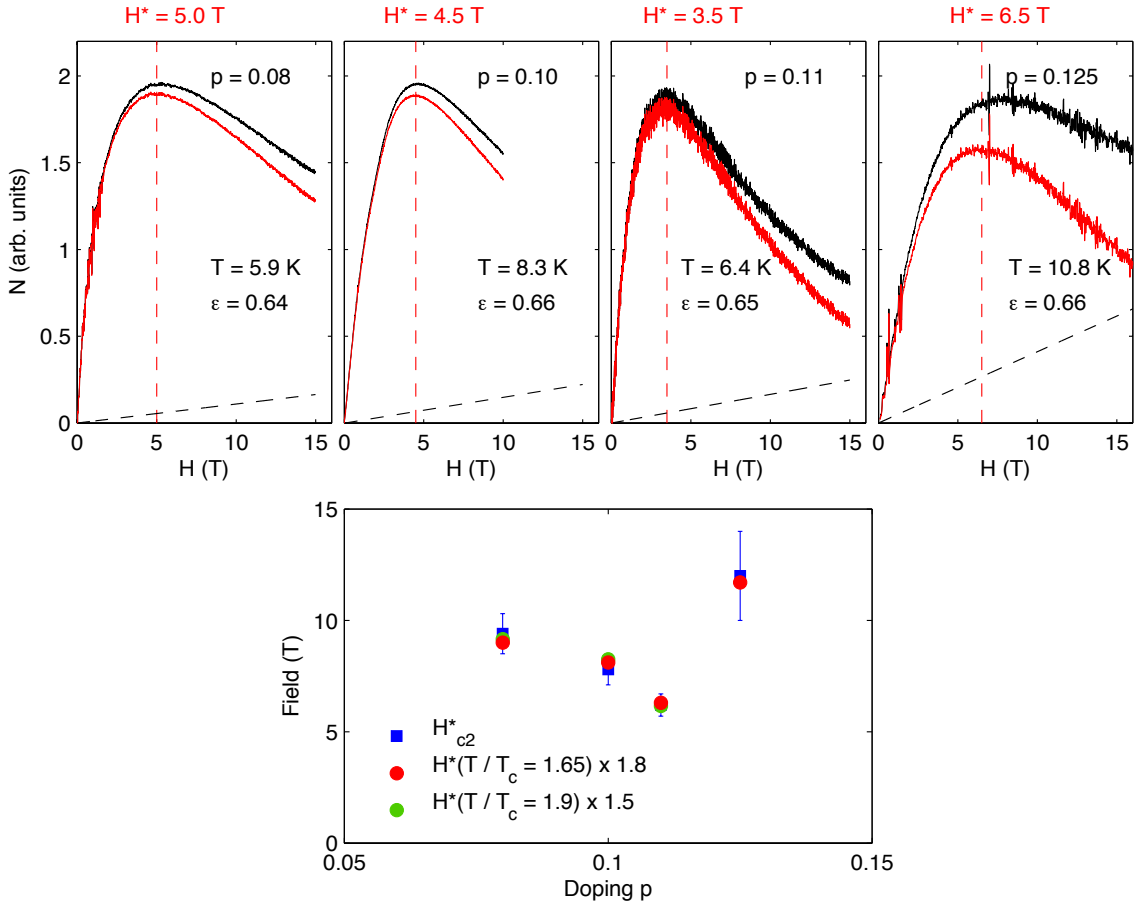

Figure S5 | Characteristic field scale of superconductivity in Eu-LSCO.

Top panels: Raw Nernst signal N (black) measured on 4 samples of Eu-LSCO with doping p as indicated, as a function of magnetic field H. In each case, the isotherm is taken at the same relative temperature T = 1.65 T_c (ε = 0.65). A small quasiparticle contribution $N_{qp} = \nu_{qp} H$ (black dashed line; Fig. 2) is subtracted to obtain $N_{sc} = N - N_{qp}$ (red), the Nernst signal from superconducting fluctuations. The peak field H^*, whose value is indicated for each doping (red dashed line), provides a simple and direct characteristic field scale for superconductivity, free of any model, theory or assumption.

Bottom panel: Doping dependence of H^* obtained at T / T_c = 1.65 (red circles; from top panels) and T / T_c = 1.9 (green circles; from Fig. S8), compared to H_{c2}^* obtained by fitting H^* vs ε to the expression $H^* = H_{c2}^* \ln(T / T_c)$ (Fig. 3) over a range of temperatures (blue squares; from Fig. 5a or Table S1).

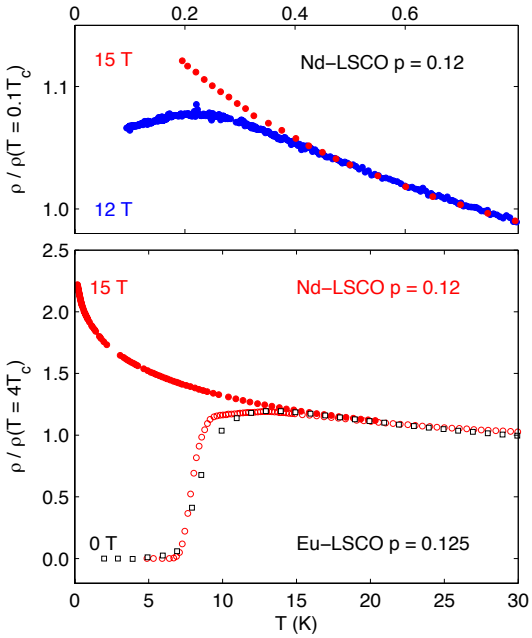

Figure S6 | Resistivity and H_{c2} of Nd-LSCO.

Temperature dependence of the in-plane electrical resistivity ρ in a single crystal of $La_{1.6-x}Nd_{0.4}Sr_xCuO_4$ (Nd-LSCO; circles), a material very similar to Eu-LSCO, for a doping p = 0.12, at three different values of the magnetic field H applied along the c axis, as indicated. Bottom panel: At H = 0 (open red circles), the superconducting transition temperature T_c, defined as the temperature where ρ → 0, is the same as in our Eu-LSCO sample with p = 0.125 (open black squares; from Fig. S3), namely $T_c \approx 7$ K.

Top panel: A zoom at very low temperature shows that the field needed to fully suppress superconductivity at $T = T_c / 20$ is 12 T. From this we conclude that the T=0 upper critical field of Nd-LSCO at that doping is close to $H_{c2} \approx 12$ T. We infer that this must also be the value of H_{c2} in Eu-LSCO at $p \approx 0.12$. This is very close to the value of H_{c2}* obtained from superconducting fluctuations in the Nernst signal above T_c in Eu-LSCO at p = 0.125 (Table S1). Resistivity data on Nd-LSCO at p = 0.20 (not shown), where T_c = 20.5 K, yield $H_{c2} \approx 35$ T (using the same criterion), so that H_{c2} falls with underdoping (Table S1).

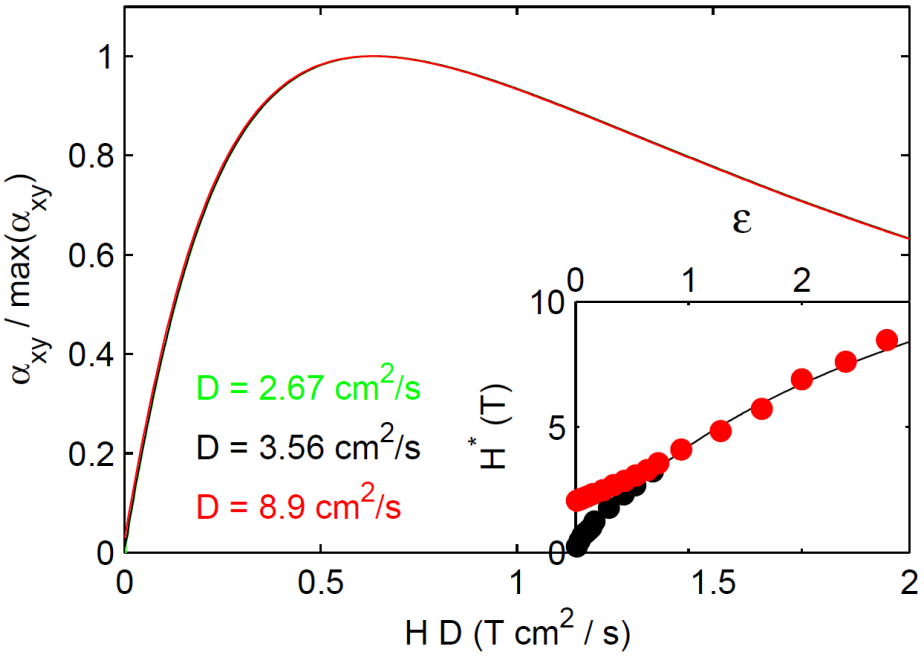

Figure S7 | Theoretical calculation of α_{xy} and *H.**

Field dependence of the Peltier coefficient $\alpha_{xy} = N_{sc}\sigma$ calculated from Gaussian fluctuation theory [15, 40] at T = 1.08 T_c, for three values of the diffusion constant D (~ ξ_0^2), as indicated [K. Michaeli, private communication]. α_{xy} is normalized by its peak value and plotted vs H D. This shows theoretically that Nernst isotherms at a given value of T / T_c from samples with different values of ξ_0 and T_c should collapse when normalized in this way. This is indeed what we find experimentally (Fig. S8). *Inset*: Comparison of the peak field H^* extracted from: 1) experimental Nernst isotherms on Eu-LSCO at p = 0.11 (red points; Fig. 3b); 2) calculated α_{xy} isotherms (black points, normalized to the experimental points at ε = 0.8). This confirms theoretically that $H^* \sim (1 / \xi_0^2) \ln(T/T_c)$. The fact that the experimental H^* deviates from the theoretical curve at low ε is an artefact of extracting H^* from N rather than from $\alpha_{xy} = N\sigma$, given that σ has strong field dependence near T_c (see Fig. S4).

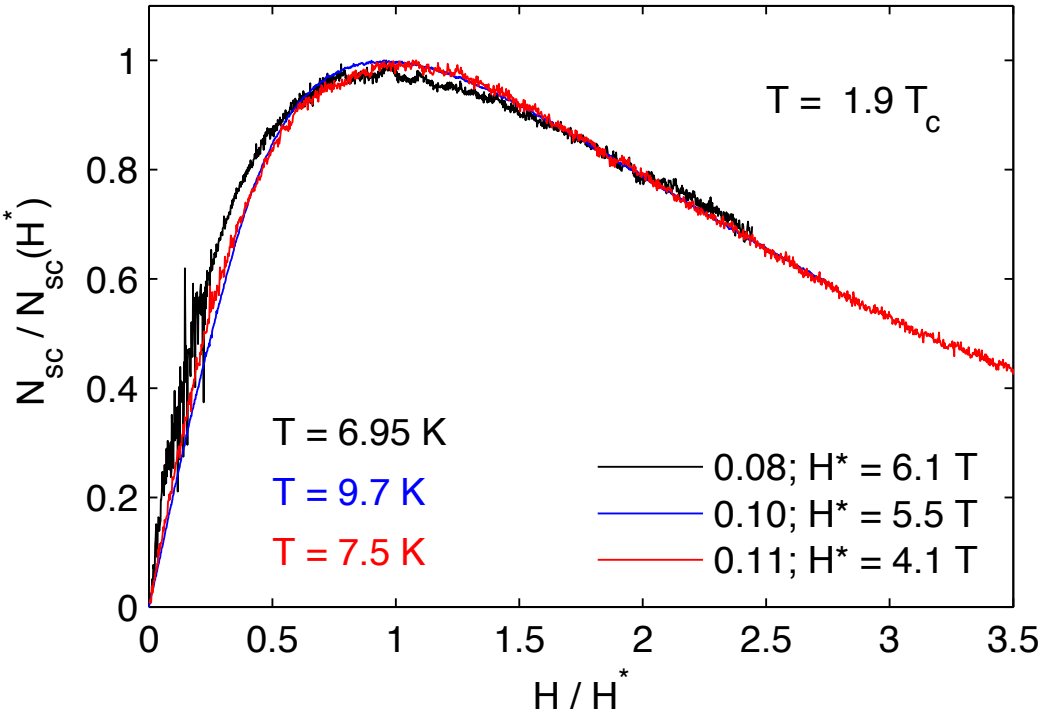

Figure S8 | Collapse of Nernst isotherms.

Superconducting Nernst signal in Eu-LSCO, plotted as $N_{sc}(H) / N_{sc}(H^*)$ vs H / H^*, for three different dopings as indicated, for the same reduced temperature $T / T_c = 1.9$ ($\varepsilon = 0.9$). H^* is the field at which N_{sc} peaks, with values as indicated. The fact that isotherms of different samples collapse onto the same curve is consistent with theoretical expectation for Gaussian fluctuations (Fig. S7). When performed at a temperature such that H-dependent paraconductivity effects are negligible (Fig. S4), as here, this scaling of Nernst isotherms at different dopings immediately reveals the doping dependence of the characteristic field scale of superconductivity (Fig. S5).

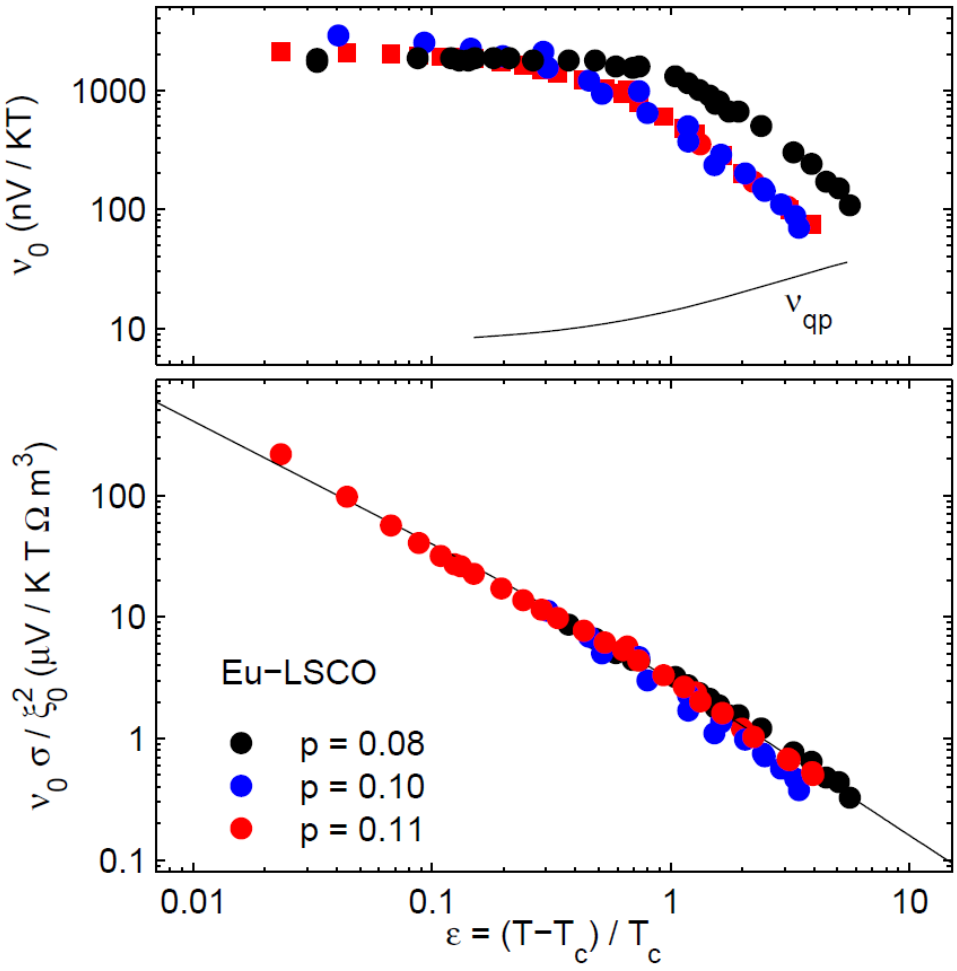

Figure S9 | Temperature dependence of low-*H* Nernst data in Eu-LSCO.

Temperature dependence of ν_0 and $\nu_0\sigma$ in Eu-LSCO with p = 0.08, 0.10, and 0.11 plotted on a log-log scale. Top panel: $\nu_0 = \nu(H\rightarrow 0)$ vs $\varepsilon = (T\text{-}T_c) / T_c$. The solid line is the quasiparticle contribution ν_{qp} (Figs. 2 and 4b). Bottom panel: $\nu_0 \sigma / \xi_0^2$ vs ε. The zero-field conductivity data σ is from Fig. S3 ($\sigma = 1/\rho$). The values of ξ_0 are obtained from $H_{c2}^* = \Phi_0 / 2\pi\xi_0^2$, with H_{c2}^* values given in Table S1. The solid line shows the temperature dependence predicted theoretically [14, 15], namely: $\nu_0 \sigma / \xi_0^2 \sim 1 / (1 + \varepsilon) \log(1 + \varepsilon)$.